Amino acid residues in the P2X7 receptor that mediate differential sensitivity to ATP and BzATP

Mark T. Young, Pablo Pelegrin and Annmarie Surprenant

Department of Biomedical Science, University of Sheffield, Addison Building Western Bank, Sheffield S10 2TN, UK

Running title: Different sites for ATP and BzATP at $P2X_7$ receptors

Corresponding author: A. Surprenant at Department of Biomedical Science, Addison Building Western Bank, University of Sheffield, Sheffield S10 2TN, UK. phone: 44-114-222-2366; fax: 44-114-222-2360
email: a.surprenant@sheffield.ac.uk

Abbreviations used: ATP, adenosine 5'-triphosphate; BzATP, 2'-3'-O-(4-benzoylbenzoyl) adenosine 5'-triphosphate; HEK293, human embryonic kidney cell line; EtBr, ethidium bromide; PVDF, polyvinylidene difluoride

Abstract

Agonist properties of the P2X7 receptor (P2X7R) differ strikingly from other P2X receptors in two main ways: high concentrations of ATP (> 100 microM) are required to activate the receptor, and the ATP analog 2',3'-O-(4-benzoyl-benzoyl)ATP (BzATP) is both more potent than ATP and evokes a higher maximum current. However, there are striking species differences in these properties. We sought to exploit the large differences in ATP and BzATP responses between rat and mouse P2X7R to delineate regions or specific residues that may be responsible for the unique actions of these agonists at the P2X7R. We measured membrane currents in response to ATP and BzATP at wild-type rat and mouse P2X7R, at chimeric P2X7Rs, and at mouse P2X7Rs bearing point mutations. Wild-type rat P2X7R was 10 times more sensitive to ATP and 100 times more sensitive to BzATP than wild-type mouse P2X7R. We found that agonist EC50 values were determined solely by the ectodomain of the P2X7R. Two segments (residues 115-136 and 282-288), when transposed together, converted mouse sensitivities to those of rat. Point mutations through these regions revealed a single residue, asparagine284, in the rat P2X7R that fully accounted for the 10-fold difference in ATP sensitivity, whereas the 100-fold difference in BzATP sensitivity required the transfer of both Lys127 and Asn284 from rat to mouse. Thus, single amino acid differences between species can account for large changes in agonist effectiveness and differentiate between the two widely used agonists at P2X7 receptors.

Introduction

P2X receptors are a seven-membered family of ATP-gated ion channels differentially expressed in both excitable and inexcitable cells (Burnstock and Knight, 2004). They are all cationic-selective ion channels bearing no sequence homology to other ATP-binding proteins, ion channels or other protein families. Each receptor subunit (from 384 residues in $P2X_4R$ to 595 residues in $P2X_7R$) has a similar membrane topology consisting of two transmembrane domains, intracellular N and C-termini and a large extracellular domain in which there are 10 fully conserved cysteines. The $P2X_7$ receptor ($P2X_7R$) is the most structurally and functionally divergent member of this family. It is the only subunit which does not heteropolymerize with other P2X receptors, it is potently inhibited by extracellular calcium and/or magnesium, and the

ion channel itself, or more likely, a distinct associated protein, dilates over several seconds to allow passage of molecules up to 900 dalton (North, 2002). But what sets this ion channel apart from all known proteins is that its activation by extracellular ATP rapidly engages a series of cytoskeletal and mitochondrial alterations which include actin/α-tubulin rearrangements, phosphatidylserine translocation, mitochondrial swelling and loss of mitochondrial membrane potential, and membrane blebbing (Mackenzie et al., 2001, 2005; Morelli et al., 2003; Verhoef et al., 2003; Pfeiffer et al., 2004; Elliott et al., 2005). All of these events occur within 2 - 30 s of maximum receptor activation, are fully reversible and do not lead to cell death unless receptor stimulation is sustained for many minutes, after which apoptosis and/or cell necrosis is inevitable (Mackenzie et al., 2001, 2005; Le Feuvre et al., 2002; Ferrari et al., 2006). The C-terminus (which is 100-200 amino acids longer than other P2XRs) is required for all these downstream signalling events but not for the initial channel opening (North, 2002). The $P2X_7R$ is prominent in immune cells of monocyte/macrophage lineage where it is up-regulated and becomes functionally active in response to inflammatory stimuli (Ferrari et al., 2006). In immune cells, $P2X_7R$ signalling cascades culminate in several physiologically significant events including processing and release of the pro-inflammatory cytokine, interleukin-1β (IL-1β), release of TNFα, NF-κB activation and killing of macrophage-engulfed *Mycobacterium tuberculosis* (North, 2002; Ferrari et al., 2006). Studies using mice in which the $P2X_7R$ has been deleted have confirmed involvement of this receptor in these processes and further support a role for $P2X_7R$ in inflammatory disease processes (Solle et al., 2001; Labasi et al., 2002; Chessell et al., 2005).

$P2X_7Rs$ also present a distinct pharmacological profile by their low affinity for ATP (> 100 μM), which is 100 - 500 fold lower than other P2X receptors, and by the several-fold higher potency of 2',3'-O-(4-benzoyl-benzoyl)ATP (BzATP) over ATP (Baraldi et al., 2004). Indeed, this BzATP:ATP potency ratio has often been used as the primary distinguishing feature of the $P2X_7R$, but it is not equally reliable among species (Surprenant et al., 1996; Chessell et al., 1998a,b; Hibell et al., 2000; Young et al., 2006). Species differences in agonist and antagonist pharmacology are unusually great for $P2X_7R$ sequences; for example, several isoquinolone derivatives such as KN-62 and KN-04 block human $P2X_7Rs$ with low nanomolar affinity but are without effect at rodent $P2X_7Rs$ even at high micromolar concentrations (Humphreys et al.,

1998; Baraldi et al., 2004). Moreover, there are distinct loss-of-function polymorphisms that have been described in the human and mouse $P2X_7R$ (Adriouch et al., 2002; Gu et al., 2004; Cabrini et al., 2005; Shemon et al., 2005). Pharmacological characterizations and structure-function studies of $P2X_7Rs$ have mainly been obtained from heterologous expression of the rat orthologue; however, increasing use of $P2X_7R$ knock-out mice in animal models of neuropathic and inflammatory pain (Chessell et al., 2005) requires a more precise knowledge of the properties of this $P2X_7R$. This is particularly important because such animal models may be of limited value if properties of agonists and antagonists are very different from human. More generally, information concerning residues involved in agonist binding to P2XRs remains fairly limited and does not extend to $P2X_7Rs$ (North, 2002; Mager et al., 2004; Roberts and Evans, 2004; Vial et al., 2004). Given the marked differences in ATP and BzATP affinity at rat $P2X_7Rs$ relative to other P2XRs, it may be expected that distinct agonist binding domains will be identified at $P2X_7Rs$. The purpose of the present study was to identify residues in mouse and rat $P2X_7Rs$ that may be involved in agonist binding, particularly those that may account for the unique BzATP:ATP affinity ratio. We recently noted a significant difference in this ratio between rat and mouse $P2X_7Rs$ (Young et al., 2006). In the present study, we have exploited this difference by way of a series of chimeric and mutagenesis experiments designed to provide insight into residues involved. We have identified two residues in the ectodomain of $P2X_7R$ that can account for the differing BzATP:ATP ratio: residue 127 which primarily influences BzATP affinity and residue 284 which influences ATP affinity.

Materials and Methods

Cell culture, transfection and site-directed mutagenesis. HEK293 cells were transiently transfected using Lipofectamine 2000 (Invitrogen, Paisley, UK). Cells were plated onto 13mm glass coverslips and maintained in Dulbecco's modified Eagle medium, supplemented with 10% heat inactivated fetal calf serum and 2mM L-glutamine at 37°C in a humidified 5% CO_2 incubator. Both rat and mouse $P2X_7$ constructs (Surprenant et al., 1996; Chessell et al., 1998b) were sub-cloned in the same expression vector background (pcDNA3, Invitrogen, Paisley, UK) and bore C-

terminal Glu-Glu epitope tags (EYMPME) to allow detection of protein expression by Western blotting. The 3' and 5'-non-coding regions of the mouse $P2X_7$ construct was engineered to be identical to that of the rat $P2X_7$ construct in order to eliminate any differences in expression due to non-coding sequences. Point mutations were generated from the above constructs using the PCR overlap extension method (Urban et al., 1997) and Accuzyme proof-reading DNA polymerase (Bioline, London, UK). Single chimeras (Fig. 2B) were produced using 21 nucleotides synthetic oligonucleotides designed with an in-frame 9 nucleotides 5'-adapter tail to introduce overlapping sequences to fuse chimeras between rat and mouse $P2X_7R$ sequences. These oligonucleotides were used in combination with the T7 sense and BGH antisense oligonucleotides annealing in the pcDNA3 expression vector sequence. Overlapping amplification products were purified from a 1% agarose gel electrophoresis and used in combination for a second PCR amplification using the T7 sense and BGH antisense oligonucleotides. Three consecutive overlapping PCR amplifications were necessary to produce double chimeras (Fig. 2B). Final T7/BGH amplified products were double-digested with *Hin*dIII and *Xba*I and replaced back in the *Hin*dIII-*Xba*I positions of the original vector. A high concentration of template vector in combination with a proof-reading DNA polymerase and a low number of cycling steps were used in all amplification reactions to minimize random mutations. All subcloned products were confirmed by sequencing (Beckman-Coulter CEQ 2000 Dye Terminator) and protein expression was verified by Western blotting.

Protein solubilisation, deglycosylation and Western blotting. Confluent cells were washed with PBS and pelleted. Cell pellets were lysed in PBS containing 1% Triton X-100 and antiproteases (Complete, Roche, Lewes, UK) for 1 hour at 4°C, followed by centrifugation at 16000 x g for 10 minutes to pellet debris. Total protein samples were removed and assayed for protein content using the Bio-Rad Protein Assay kit (Bio-Rad, Hemel Hempstead, UK). SDS-PAGE sample buffer was added and the samples were boiled for 2 minutes at 100°C to denature the protein. Where appropriate, deglycosylation was performed by incubating protein samples (100μg) for 1 hour at 37ºC with 500 units of PNGase F (NEB, Herts, UK) according to the manufacturer's instructions. Samples were separated on 8% polyacrylamide gels according to standard methods (Laemmli, 1970) and transferred to PVDF membranes. Western blotting was performed according to standard protocols and proteins were

visualised using anti Glu-Glu primary antibody (Bethyl Laboratories, Cambridge, UK) and HRP-conjugated secondary antibody (DA-KOCytomation, Ely, UK), both at 1:2000 dilution, followed by detection using the ECL-plus kit (Amersham, Bucks, UK) and Kodak Bio-Max MS film (Sigma, Poole, UK).

Electrophysiological recordings. Whole-cell recordings were made 24-48 hours after transfection using an EPC9 patch clamp amplifier (HEKA Electronik, Lambrecht, Germany). Membrane potential was held at –60mV. Recording pipettes (5-7 MΩ) were pulled from borosilicate glass (World Precision Instruments, Sarasota, Florida) and filled with an intracellular solution that consisted of (in mM): 145 NaCl, 10 ethylene glycol-bis-(2-aminoethyl ether)-*N,N,N',N'*-tetraacetic acid (EGTA), 10 N-2-hydroxyethylpiperazine-N'-2-ethanesulphonic acid (HEPES). The external solution contained (in mM): 147 NaCl, 10 HEPES, 13 glucose, 2 KCl, 2 $CaCl_2$, 1 $MgCl_2$. Agonists were applied in solution containing low divalent cation concentrations which consisted of (in mM): 147 NaCl, 10 HEPES, 13 glucose, 2 KCl; cells were otherwise superfused with normal external solution. Osmolarity and pH values of all solutions were 295-310 mOsM/l and 7.3 respectively. All experiments were performed at room temperature. Agonists were applied using a RSC 200 fast-flow delivery system (BioLogic Science Instruments, Grenoble, France). Agonists were applied for 5- or 10-second duration to obtain steady-state responses. Concentration-response curves to ATP and BzATP were obtained by first obtaining a maximum response to agonist, as marked run-up of response was observed at both rat and mouse $P2X_7$ receptors, (Surprenant et al., 1996; Chessell et al., 1998b; Young et al., 2006), and then either applying decreasing or increasing concentrations. In either case, similar curves were obtained, provided that a maximum response had been obtained beforehand. All experiments were performed at a holding potential of -60 mV. Concentration-response curves were plotted using KaleidaGraph (Synergy Software, Reading, Pennsylvania) and Prism v3.0a Software (Graphpad Prism; www.graphpad.com) using the Hill equation provided in Prism.

Results

Comparison of mouse and rat $P2X_7$ receptors. Although all $P2X_7$Rs are potently inhibited by extracellular divalent cations, there is a significant species difference with Mg^{++} and Ca^{++} being approximately 10-fold more potent to inhibit

human than rat $P2X_7Rs$ (Surprenant et al., 1996; Rassendren et al., 1997). In preliminary experiments, we found that mouse $P2X_7R$ was also more sensitive (by approximately 5-fold) to inhibition by Mg^{++} and Ca^{++} than was rat $P2X_7R$ (data not shown). Therefore, all agonist responses were recorded in the low divalent cation solution in order to rule out possible contributions of differential divalent cation sensitivity to agonist concentration-responses. We first compared ATP and BzATP concentration-response curves from wildtype rat and mouse $P2X_7Rs$, using equal amounts of cDNA for transfection, and using a 10-fold lower concentration of $rP2X_7R$ cDNA which we have previously found results in similar protein expression of rat and mouse $P2X_7Rs$ (Young et al., 2006). Typical currents recorded from cells transfected with equal cDNA concentrations are shown in Fig. 1A and results from all experiments are shown in Fig. 1B, C. Reducing the $rP2X_7R$ cDNA concentration by 10-fold resulted in approximately 50% reduction in maximum currents to ATP or BzATP (Fig. 1B) without a significant change in agonist EC_{50} values or BzATP:ATP maximum current ratio or EC_{50} ratio (Fig. 1D, E). The maximum agonist-evoked currents recorded from cells transfected with $mP2X_7R$ were approximately the same as those recorded from cells transfected with the 10-fold lower $rP2X_7R$ cDNA concentration (Fig. 1B). In agreement with earlier studies on human and rat $P2X_7Rs$ (Surprenant et al., 1996; Wiley et al., 1998; Hibell et al., 2000), we found ATP to be a partial agonist relative to BzATP, with maximum BzATP-evoked currents that were 30 - 45% greater than maximum ATP-evoked currents at both rat and mouse $P2X_7R$ (Fig. 1D). EC_{50} values for BzATP and ATP at the rat $P2X_7R$ (3.6 μM and 123 μM, respectively) were several-fold lower than at the mouse $P2X_7R$ (285 μM and 936 μM) (Table 1). These values yield a striking difference in the BzATP:ATP EC_{50} ratio, which was 34 at the $rP2X_7R$ but only 3.3 at the mouse $P2X_7R$ (Fig. 1E).

Chimeric substitutions of rat $P2X_7R$ segments into mouse $P2X_7R$. Rat and mouse $P2X_7R$ sequences are 84% identical with 88 specific amino acid differences; most of the non-conservative differences are found in two distinct regions of the ectodomain or in the intracellular C-terminal domain (Fig. 2A). Of the 22 non-conserved amino acids in the ectodomain, 8 are found in the region ecompassing residues 115-136, 4 are found between residues 282 and 288 and the remaining half are scattered throughout the extracellular loop (Fig. 2A). We therefore made a series of chimeric constructs depicted in Fig. 2B in order to examine the effects of

transposing rat ectodomain, C-terminus, residues 115-136 and 282-288 (alone and in combination) into the mouse $P2X_7R$ on agonist-evoked responses.

Neither agonist concentration-response curves nor agonist-evoked kinetics were altered by transposing rat intracellular C-terminus onto mouse $P2X_7R$, or vice versa (Fig. 3A, C). Transposition of rat ectodomain onto mouse $P2X_7R$ resulted in ATP and BzATP EC_{50} values that were the same as for wildtype rat $P2X_7R$ (Fig. 3C) but deactivation kinetics were several-fold slower (Fig. 3B). No responses were recorded from cells in which the mouse ectodomain was transposed into the rat $P2X_7R$. The chimeric mouse $P2X_7R$ containing residues 115-136 of rat $P2X_7R$ resulted in a pronounced leftward shift of the BzATP concentration response curve without any alteration in the ATP-evoked responses (Fig. 4A; Table 1). When residues 282-288 of rat $P2X_7R$ were inserted into mouse $P2X_7R$, there was a small leftward shift in the BzATP concentration-response curve but a large leftward shift in the ATP concentration response (Fig. 4B; Table 1). Substitution of both regions of rat $P2X_7R$ into mouse $P2X_7R$ resulted in agonist-evoked concentration-response curves and EC_{50} values that were not significantly different from wildtype rat $P2X_7R$ (Fig. 4C; Table 1).

Point mutations into mouse $P2X_7R$. We next substituted individually each rat $P2X_7R$ residue in these regions into the mouse receptor, and examined agonist responses in these mutant receptors. ATP-evoked responses were not different from wildtype mouse $P2X_7R$ for any mutation except at residue 284, where substitution of asparagine (rat $P2X_7R$) for aspartate (mouse $P2X_7R$) resulted in ATP concentration response and EC_{50} that was not significantly different from wildtype rat $P2X_7R$ (Fig. 5A; Table 1). In contrast, BzATP EC_{50} values were significantly lower than wildtype mouse $P2X_7R$ in cells expressing any one of the following point mutants: D284N ($p < 0.01$); A127K ($p < 0.01$), S130K ($p < 0.1$), R134G ($p < 0.05$) and K136I ($p < 0.05$), with the A127K mutation showing the largest difference (BzATP EC_{50} = 80 μM vs 3.6 μM at rat $P2X_7R$ and 285 μM at mouse $P2X_7R$) (Fig. 5B; Table 1). We therefore examined agonist responses at the double mutant m$P2X_7R$-A127K/D284N and found that neither ATP nor BzATP EC_{50} concentrations were significantly different from wildtype rat $P2X_7R$ (Fig. 5A,B; Table 1). One striking difference between responses at the mouse $P2X_7R$-A127K/D284N and the wildtype rat $P2X_7R$ was that the BzATP:ATP I_{max} ratio was reversed at this double mutant; that is, while maximum

BzATP-evoked currents were approximately 30% greater than maximum ATP-evoked currents at both mouse and rat $P2X_7R$ (Fig. 1D) the ATP-evoked currents were 36 ± 5% (n = 5) greater than maximum BzATP-evoked currents at the mouse $P2X_7R$-A127K/D284N receptor.

The substitution of Asp^{284} with asparagine at the mouse $P2X_7R$ generates a potential N-glycosylation acceptor sequence (NESF). The wildtype rat $P2X_7R$ also contains a similar potential acceptor sequence at this position (NESL). Because it has been well demonstrated at other P2XRs that adding N-glycosylation sites significantly increases, while removing N-glycosylation sites decreases, protein expression (Newbolt et al., 1998; Torres et al., 1998; Rettinger et al., 2001; Chaumont et al., 2004), we assayed protein expression in wildtype, chimeric and m$P2X_7$D284N receptor and asked whether this site was, indeed, glycosylated. As found previously (Young et al., 2006), transfection with equal concentrations of rat and mouse $P2X_7R$ cDNA yielded protein level ratios of approximately 3:1 (Fig. 6A). The presence of rat $P2X_7R$ ectodomain, but not N-terminus, C-terminus nor transmembrane domains, yielded protein levels not significantly different from wildtype rat $P2X_7R$, while presence of mouse ectodomain yielded low protein expression equivalent to wildtype mouse $P2X_7R$ (Fig. 6A). We then removed N-glycan chains from wildtype mouse and rat $P2X_7R$ and mouse $P2X_7$-D284N receptor using PNGase F and examined molecular mass by SDS-PAGE. Wildtype rat $P2X_7R$, mouse $P2X_7$-D284N receptor, and mouse $P2X_7R$ bands were detected at 78 kDa, 78 kDa and 75 kDa respectively (Fig. 6B). After PNGase F treatment all receptors were detected at approximately 65 kDa (Fig. 6B).

DISCUSSION

Points

Main new results/insight into p2X7 structure-function: Sites involved with ATP and BzATP responses are different, and also these sites are unique to P2X7 and may explain striking agonist potency differences between P2X7 and all other P2XRs. N284 (in rat) definitely determines species differences in regard to ATP sensitivity. The mouse D284N receptor showed (exactly!) the same ATP responses (kinetics, maximum current, EC50) as did wildtype rat P2X7R. BzATP sensitivity seems to be a function mainly (but not solely) of K127 (in rat) but it is more likely to be due to a

cooperative actions of residues between 127 and 136 (as these all decreased BzATP EC50 values).

The D284N can fully account for ATP differential but only partially for the BzATP differential,with additional residues (mainly 127K) contributing to the BzATP potency. Possible explanation. residue 284 takes part in both ATP and BzATP binding (at this residue or at other residues) while residue 127 (and other residues in this region that show some contribution) takes part only in BzATP binding (at these or other residues).

How this relates to models (from Evans/North/Crazy Russian) of agonist binding at other P2X R. Brief mention of N-glycoslyation altering agonist binding in other P2X – Rettinger et al 2001 so this may be expected – another reason why mouse may not be such good model. [Set of expts to do: just how many N-glycan sites in human are there – what is effect of removing/adding any]

How this advances our understanding of P2X7R pharmacology – (SAR on BzATP?)

References

Adriouch S, Dox C, Welge V, Seman M, Koch-Notle F, and Haag F (2002) Cutting edge: a natural P451L mutation in the cytoplasmic domain impairs the function of the mouse P2X7 receptor. *J Immunol* **169:**4108-4112.

Baraldi PG, Di Virgilio F, and Romagnoli R (2004) Agonists and antagonists acting at P2X7 receptor. *Curr Top Med Chem* **4:**1707-1717.

Burnstock G and Knight GE (2004) Cellular distribution and functions of P2 receptor subtypes in different systems. *Int Rev Cytol* **240**:31-304.

Cabrini G, Falzoni S, Forchap SL, Pellegatti P, Balboni A, Agostini P, Cuneo A, Castoldi G, Baricordi OR, and Di Virgilio F (2005) A His-155 to Tyr polymorphism confers gain-of-function to the human P2X7 receptor of human leukemic lymphocytes. *J Immunol* **175**(1):82-89.

Chaumont S, Jiang LH, Penna A, North RA, and Rassendren F (2004) Identification of a trafficking motif involved in the stabilization and polarization of P2X receptors. *J Biol Chem* **279**(28):29628-29638.

Chessell IP, Hatcher JP, Bountra C, Michel AD, Hughes JP, Green P, Egerton J, Murfin M, Richardson J, Peck WL, Grahames CB, Casula MA, Yiangou Y, Birch R, Anand P, and Buell GN (2005) Disruption of the P2X7 purinoceptor

gene abolishes chronic inflammatory and neuropathic pain. *Pain* **114**(3):386-396.

Chessell IP, Michel AD, and Humphrey PP (1998a) Effects of antagonists at the human recombinant P2X7 receptor. *Br J Pharmacol* **124**(6):1314-1320.

Chessell IP, Simon J, Hibell AD, Michel AD, Barnard EA, and Humphrey PP (1998b) Cloning and functional characterisation of the mouse P2X7 receptor. *FEBS Lett* **439**(1-2):26-30.

Elliott JI, Surprenant A, Marelli-Berg FM, Cooper JC, Cassady-Cain RL, Wooding C, Linton K, Alexander DR, and Higgins CF (2005) Membrane phosphatidylserine distribution as a non-apoptotic signalling mechanism in lymphocytes. *Nat Cell Biol* **7**(8):808-816.

Ferrari D, Pizzirani C, Adinolfi E, Lemoli RM, Curti A, Idzko M, Panther E, and Di Virgilio F (2006) The P2X7 receptor: a key player in IL-1 processing and release. *J Immunol* **176:**3877-3883.

Gu BJ, Sluyter R, Skarratt KK, Shemon AN, Dao-Ung LP, Fuller SJ, Barden JA, Clarke AL, Petrou S, and Wiley JS (2004) An Arg307 to Gln polymorphism within the ATP-binding site causes loss of function of the human P2X7 receptor. *J Biol Chem* **279**(30):31287-31295.

Guerra AN, Fisette PL, Pfeiffer ZA, Quinchia-Rios BH, Prabhu U, Aga M, Denlinger LC, Guadarrama AG, Abozeid S, Sommer JA, Proctor RA, and Bertics PJ (2003) Purinergic receptor regulation of LPS-induced signaling and pathophysiology. *J Endotoxin Res* **9**(4):256-263.

Haines WR, Migita K, Cox JA, Egan TM, and Voigt MM (2001) The first transmembrane domain of the P2X receptor subunit participates in the agonist-induced gating of the channel. *J Biol Chem* **276**(35):32793-32798.

Hibell AD, Kidd EJ, Chessell IP, Humphrey PP, and Michel AD (2000) Apparent species differences in the kinetic properties of $P2X_7$ receptors. *Br J Pharmacol* **130**(1):167-173.

Humphreys BD, Virginio C, Surprenant A, Rice J, and Dubyak G (1998) Isoquinolines as antagonists of the P2X7 nucleotide receptor: high selectivity for the human versus rat receptor homologues. *Mol Pharmacol.* **54:**22-32.

Labasi JM, Petrushova N, Donovan C, McCurdy S, Lira P, Payette MM, Brissette W, Wicks JR, Audoly L, and Gabel CA (2002) Absence of the $P2X_7$ receptor

alters leukocyte function and attenuates an inflammatory response. *J Immunol* **168**(12):6436-6445.

Laemmli UK (1970) Cleavage of structural proteins during the assembly of the head of bacteriophage T4. *Nature* **227**(5259):680-685.

Le Feuvre RA, Brough D, Iwakura Y, Takeda K, and Rothwell NJ (2002) Priming of macrophages with lipopolysaccharide potentiates P2X7-mediated cell death via a caspase-1-dependent mechanism, independently of cytokine production. *J Biol Chem* **277**(5):3210-3218.

Le Novere N, Grutter T, and Changeux JP (2002) Models of the extracellular domain of the nicotinic receptors and of agonist- and Ca2+-binding sites. *Proc Natl Acad Sci U S A* **99**(5):3210-3215.

MacKenzie A, Wilson HL, Kiss-Toth E, Dower SK, North RA, and Surprenant A (2001) Rapid secretion of interleukin-1beta by microvesicle shedding. *Immunity* **15**(5):825-835.

Mackenzie AB, Young MT, Adinolfi E, and Surprenant A (2005) Pseudoapoptosis induced by brief activation of ATP-gated P2X7 receptors. *J Biol Chem* **280**(40):33968-33976.

Mager PP, Weber A, and Illes P (2004) Bridging the gap between structural bioinformatics and receptor research: the membrane-embedded, ligand-gated P2X glycoprotein receptor. *Curr Top Med Chem* **4:**1657-17705.

Maksay G, Simonyi M, and Bikadi Z (2004) Subunit rotation models activation of serotonin 5-HT3AB receptors by agonists. *J Comput Aided Mol Des* **18**(10):651-664.

Morelli A, Chiozzi P, Chiesa A, Ferrari D, Sanz JM, Falzoni S, Pinton P, Rizzuto R, Olson MF, and Di Virgilio F (2003) Extracellular ATP causes ROCK I-dependent bleb formation in $P2X_7$ transfected HEK293 cells. *Mol Biol Cell* **14:**2655-2664.

Newbolt A, Stoop R, Virginio C, Surprenant A, North RA, Buell G, and Rassendren F (1998) Membrane topology of an ATP-gated ion channel (P2X receptor). *J Biol Chem***273:**15177-15182.

North RA (2002) Molecular physiology of P2X receptors. *Physiol Rev* **82**(4):1013-1067.

Pfeiffer ZA, Aga M, Prabhu U, Watters JJ, Hall DJ, and Bertics PJ (2004) The nucleotide receptor P2X7 mediates actin reorganization and membrane

blebbing in RAW 264.7 macrophages via p38 MAP kinase and Rho. *J Leukoc Biol* **75**(6):1173-1182.

Rassendren F, Buell GB, Virginion C, Collo G, North RA, and Surprenant A (1997) The permeabilizing ATP receptor, P2X7, Cloning and expression of a human cDNA. *J Biol Chem* **272:**5482-5486.

Rettinger J, Aschrafi A, and Schmalzing G (2000) Roles of individual N-glycans for ATP potency and expression of the rat P2X1 receptor. *J Biol Chem* **275**(43):33542-33547.

Roberts JA and Evans RJ (2004) ATP binding at human P2X1 receptors. Contribution of aromatic and basic amino acids revealed using mutagenesis and partial agonists. *J Biol Chem* **279**(10):9043-9055.

Shemon AN, Sluyter R, Fernando SL, Clarke AL, Dao-Ung LP, Skarratt KK, Saunders BM, Tan KS, Gu BJ, Fuller SJ, Britton WJ, Petrou S, and Wiley JS (2005) A Thr357 to Ser polymorphism in homozygous and compound heterozygous subjects causes absent or reduced P2X7 function and impairs ATP-induced mycobacterial killing by macrophages. *J Biol Chem*. **281**:2079-2086.

Solle M, Labasi J, Perregaux DG, Stam E, Petrushova N, Koller BH, Griffiths RJ, and Gabel CA (2001) Altered cytokine production in mice lacking P2X(7) receptors. *J Biol Chem* **276**(1):125-132.

Suh BC, Kim JS, Namgung U, Ha H, and Kim KT (2001) P2X7 nucleotide receptor mediation of membrane pore formation and superoxide generation in human promyelocytes and neutrophils. *J Immunol* **166**(11):6754-6763.

Surprenant A, Rassendren F, Kawashima E, North RA, and Buell G (1996) The cytolytic P2Z receptor for extracellular ATP identified as a P2X receptor (P2X7). *Science* **272**(5262):735-738.

Torres GE, Egan TM, and Voigt MM (1998) N-Linked glycosylation is essential for the functional expression of the recombinant P2X2 receptor. *Biochemistry* **37**(42):14845-14851.

Torres GE, Egan TM, and Voigt MM (1999) Identification of a domain involved in ATP-gated ionotropic receptor subunit assembly. *J Biol Chem* **274**(32):22359-22365.

Urban A, Neukirchen S, and Jaeger KE (1997) A rapid and efficient method for site-directed mutagenesis using one-step overlap extension PCR. *Nucleic Acids Res* **25**(11):2227-2228.

Verhoef PA, Estacion M, Schilling W, and Dubyak GR (2003) P2X7 receptor-dependent blebbing and the activation of Rho-effector kinases, caspases, and IL-1 beta release. *J Immunol* **170**(11):5728-5738.

Vial C, Roberts JA, and Evans RJ (2004) Molecular properties of ATP-gated P2X receptor ion channels. *Trends Pharmacol Sci* **25:**487-493.

Wiley JS, Gargett CE, Zhang W, Snook MB, and Jamieson GP (1998) Partial agonists and antagonists reveal a second permeability state of human lymphocyte P2Z/P2X7 channel. *Am J Physiol* **275:**C1224-1231.

Young MT, Pelegrin P, and Surprenant A (2006) Identification of Thr283 as a key determinant of P2X7 receptor function. *Br J Pharmacol* (------).

Zemkova H, He ML, Koshimizu TA, and Stojilkovic SS (2004) Identification of ectodomain regions contributing to gating, deactivation, and resensitization of purinergic P2X receptors. *J Neurosci* **24**(31):6968-6978.

Table 1: EC_{50} values and Hill coefficients for all $P2X_7$ constructs used in this study.

Construct	ATP EC_{50} (μM)	h_{ATP}	BzATP EC_{50} (μM)	h_{BzATP}
$rP2X_7$ 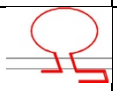	123 ± 4 (21)	1.8 ± 0.1	3.6 ± 0.2 (19)	1.8 ± 0.1
$mP2X_7$ 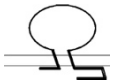	936 ± 21 (18)	1.6 ± 0.1	285 ± 16 (18)	1.6 ± 0.1
$rP2X_7$1-356 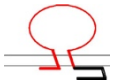	125 ± 10 (5)	1.5 ± 0.2	2.2 ± 0.2 (5)	2.2 ± 0.3
$rP2X_7$356-595 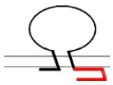	1251 ± 202 (5)	1.3 ± 0.2	306 ± 24 (3)	1.7 ± 0.2
$rP2X_7$47-334 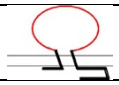	58 ± 0.8 (5)	2.1 ±0.1	1.4 ± 0.1 (5)	2.5 ± 0.1
$rP2X_7$115-136 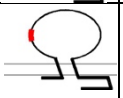	634 ± 27 (5)	1.3 ± 0.1	33 ± 2.4 (5)	1.6 ± 0.2
$mP2X_7$A127K	815 ± 56 (10)	1.0 ± 0.1	80 ± 7 (9)	1.8± 0.1
$rP2X_7$282-288 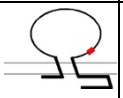	162 ± 11 (9)	1.7 ± 0.2	89 ± 4 (9)	2.0 ± 0.1
$mP2X_7$D284N	146 ± 11 (8)	1.6 ± 0.2	94 ± 7 (10)	1.2 ± 0.1
$rP2X_7$115-136 + 282-288 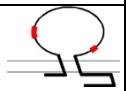	74 ± 5 (8)	2.0 ± 0.2	2.9 ± 0.1 (9)	1.7 ± 0.1
$mP2X_7$A127K/D284N	112 ± 11 (5)	1.7 ± 0.2	5 ± 1 (6)	1.6 ± 0.2

h, Hill coefficient.

Figure legends.

Figure 1. Comparison of agonist actions at wildtype rat and mouse $P2X_7R$. A, Representative currents recorded from cells expressing rat or mouse $P2X_7R$ as indicated in response to increasing concentrations of ATP or BzATP as indicated. B, Summary of all experiments as illustrated in A for wildtype rat $P2X_7R$ for cells in which standard cDNA concentration (1 μg/ml, filled symbols) or 10-fold lower concentration (0.1 μg/ml, open symbols) was used for transfection. C, Agonist concentration-response curves obtained for wildtype mouse $P2X_7R$. D, Mean ratio of maximum current amplitudes to BzATP relative to ATP shown for rat and mouse $P2X_7R$; these were similar for both species and for low and high expression levels. E, Mean ratio of EC_{50} values of BzATP relative to ATP; low or high expression of rat $P2X_7R$ showed the same approximate 36-fold difference while mouse $P2X_7R$ showed only 4-fold difference.

Figure 2. Rat and mouse $P2X_7R$ sequence alignment and design of experimental approach. A, Amino acid differences between species are shown in bold type; transmembrane domains indicated by black lines; boxed residues show regions of highest concentration of non-conservation in the ectodomain. B, Schematic representation of chimeras where red and black represent rat and mouse $P2X_7R$ sequence respectively, and are shown in this, and all subsequent figures, as rat $P2X_7R$ residues inserted into mouse $P2X_7R$ background.

Figure 3. Ectodomain is solely responsible for agonist potency at $P2X_7R$. A,B, Examples of currents recorded from rat $P2X_7R$ containing mouse C-terminus (A) and from mouse $P2X_7R$ containing rat ectodomain (B). Note the prolonged deactivation kinetics upon removal of BzATP at the mouse $P2X_7R$ containing rat ectodomain (B); no other chimeric or mutant receptor showed altered kinetics of onset or offset. C, Summary of EC_{50} values for ATP and BzATP obtained from chimeric receptors; note difference in x-axis scale for BzATP.

Figure 4. Different regions in $P2X_7R$ ectodomain determine ATP and BzATP potency. A – C, concentration-response curves for ATP (left hand graphs) and BzATP (right hand graphs) from wildtype rat $P2X_7R$ (filled circles), mouse $P2X_7R$

(filled squares) and chimeric receptors (open circles). A, When residues 115-136 from rat $P2X_7R$ were inserted into mouse $P2X_7R$, no change in ATP-evoked responses occurred while BzATP response showed a 10-fold leftward shift. B, Insertion of rat $P2X_7R$ residues 282-288 resulted in a significant leftward shift in both agonist concentration-response curves with the most pronounced effect occurring for the ATP dose-response curve. C, Insertion of both these regions of rat $P2X_7R$ into mouse $P2X_7R$ resulted in ATP concentration-response that was shifted to the left of wildtype rat $P2X_7R$ and a BzATP response that was not different from wildtype rat $P2X_7R$.

Figure 5. Asparagine^{284} governs ATP potency and lysine^{127} primarily governs BzATP potency at $P2X_7R$. Histograms of ATP (A) and BzATP (B) EC_{50} values obtained from mouse $P2X_7R$ carrying point mutations in the regions between 115-136 and 282-288. In each case the residue substituted was that found in wildtype rat $P2X_7R$. Stippled bars indicate values significantly different from wildtype $mP2X_7R$. A, ATP EC_{50} at $mP2X_7$-D284N was shifted 10-fold to the left of wildtype $mP2X_7R$ and was not significantly different from wildtype rat $P2X_7R$ while the BzATP EC_{50} was shifted only 1.6-fold to the left at this mutation. B, Mutations at residues 127, 130, 134 and 136 also shifted the BzATP EC_{50} significantly to the left with A127K mutation showing the largest effect. The mouse $P2X_7$-A127K/D284N double mutation yielded agonist EC_{50} values that were not significantly different from wildtype rat $P2X_7R$. C, Histograms of BzATP:ATP EC_{50} ratios for chimeric and mutant receptors as indicated. Ratios were similar to wildtype rat $P2X_7R$ only when both A127K and D284N mutations were present.

Figure 6. Protein expression and N-linked glycosylation at mouse and rat $P2X_7Rs$. A, Total protein expression of constructs as illustrated. Equal protein (10 μg) was loaded per lane and confirmed by comparing β-actin levels. $P2X_7R$ protein was detected using the anti-glu-glu epitope tag antibody. The ectodomain, but not transmembrane or intracellular domains, determined levels of $P2X_7R$ protein expression. B, Western blot of native and deglycosylated receptors. Both rat $P2X_7R$ and mouse $P2X_7R$-D284N exhibited higher molecular weight bands (78 kDa) than mouse $P2X_7R$ (75 kDa). Treatment with PNGase F gave rise to products of the same

lower mass of approximately 65 kDa, with an additional lower mass band (at 60 kDa) that may be due to protein degradation. C, Schematic indicating the two important residues conferring ATP (284N) and BzATP (127K) sensitivity at $P2X_7Rs$.

FIGURE 1

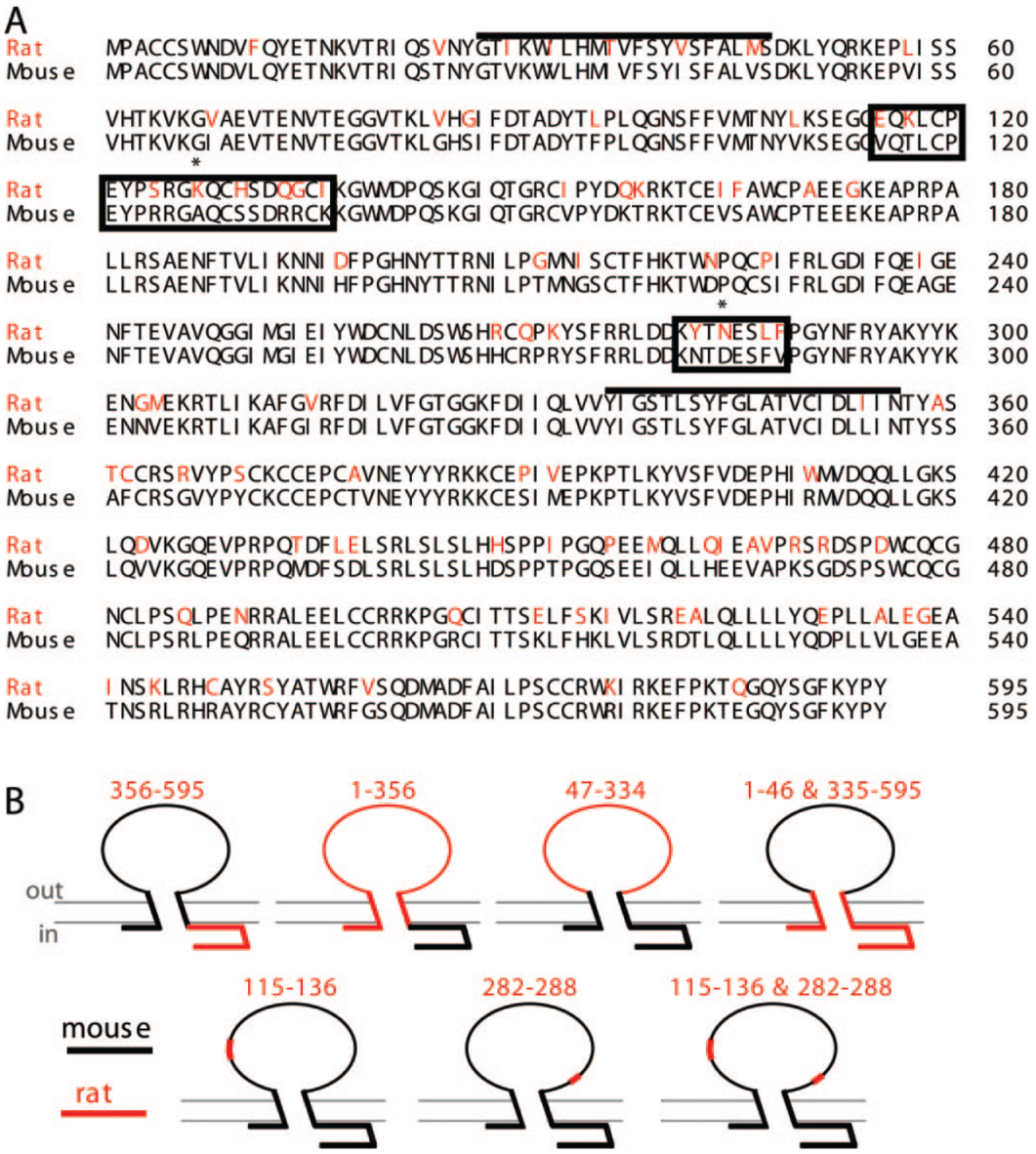
A
Rat MPACCSWNDVFQYETNKVTRIQSVNYGTTKWTLHMTVFSYVSFALMSDKLYQRKEPLISS 60
Mouse MPACCSWNDVLQYETNKVTRIQSTNYGTVKWWLHMIVFSYISFALVSDKLYQRKEPVISS 60
Rat VHTKVKGVAEVTENVTEGGVTKLVHGIFDTADYTLPLQGNSFFVMTNYLKSEGQEQKLCP 120
Mouse VHTKVKGIAEVTENVTEGGVTKLGHSIFDTADYTFPLQGNSFFVMTNYVKSEGQVQTLCP 120
Rat EYPSRGKQCHSDQGCTKGWVDPQSKGIQTGRCIPYDQKRKTCEIFAWCPAEEGKEAPRPA 180
Mouse EYPRRGAQCSSDRRCKKGWVDPQSKGIQTGRCVPYDKTRKTCEVSAWCPTEEEKEAPRPA 180
Rat LLRSAENFTVLIKNNIDFPGHNYTTRNILPGMNISCTFHKTWNPQCPIFRLGDIFQEIGE 240
Mouse LLRSAENFTVLIKNNIHFPGHNYTTRNILPTMNGSCTFHKTWDPQCSIFRLGDIFQEAGE 240
Rat NFTEVAVQGGIMGIEIYWDCNLDSWSHRCQPKYSFRRLDDKYTNESLPPGYNFRYAKYYK 300
Mouse NFTEVAVQGGIMGIEIYWDCNLDSWSHHCRPRYSFRRLDDKNTDESFVPGYNFRYAKYYK 300
Rat ENGMEKRTLIKAFGVRFDILVFGTGGKFDIIQLVVYIGSTLSYFGLATVCIDLIINTYAS 360
Mouse ENNVEKRTLIKAFGIRFDILVFGTGGKFDIIQLVVYIGSTLSYFGLATVCIDLLINTYSS 360
Rat TCCRSRVYPSCKCCEPCAVNEYYYRKKCEPIVEPKPTLKYVSFVDEPHIWMVDQQLLGKS 420
Mouse AFCRSGVYPYCKCCEPCTVNEYYYRKKCESIMEPKPTLKYVSFVDEPHIRMVDQQLLGKS 420
Rat LQDVKGQEVPRPQTDFLELSRLSLSLHHSPPIPGQPEEMQLLQIEAVPRSRDSPDWCQCG 480
Mouse LQVVKGQEVPRPQMDFSDLSRLSLSLHDSPPTPGQSEEIQLLHEEVAPKSGDSPSWCQCG 480
Rat NCLPSQLPENRRALEELCCRRKPGQCITTSELFSKIVLSREALQLLLLYQEPLLALEGEA 540
Mouse NCLPSRLPEQRRALEELCCRRKPGRCITTSKLFHKLVLSRDTLQLLLLYQDPLLVLGEEA 540
Rat INSKLRHCAYRSYATWRFVSQDMADFAILPSCCRWKIRKEFPKTQGQYSGFKYPY 595
Mouse TNSRLRHRAYRCYATWRFGSQDMADFAILPSCCRWRIRKEFPKTEGQYSGFKYPY 595
B
356-595
1-356
47-334
1-46 & 335-595
out
in
115-136
282-288
115-136 & 282-288
mouse
rat

FIGURE 2

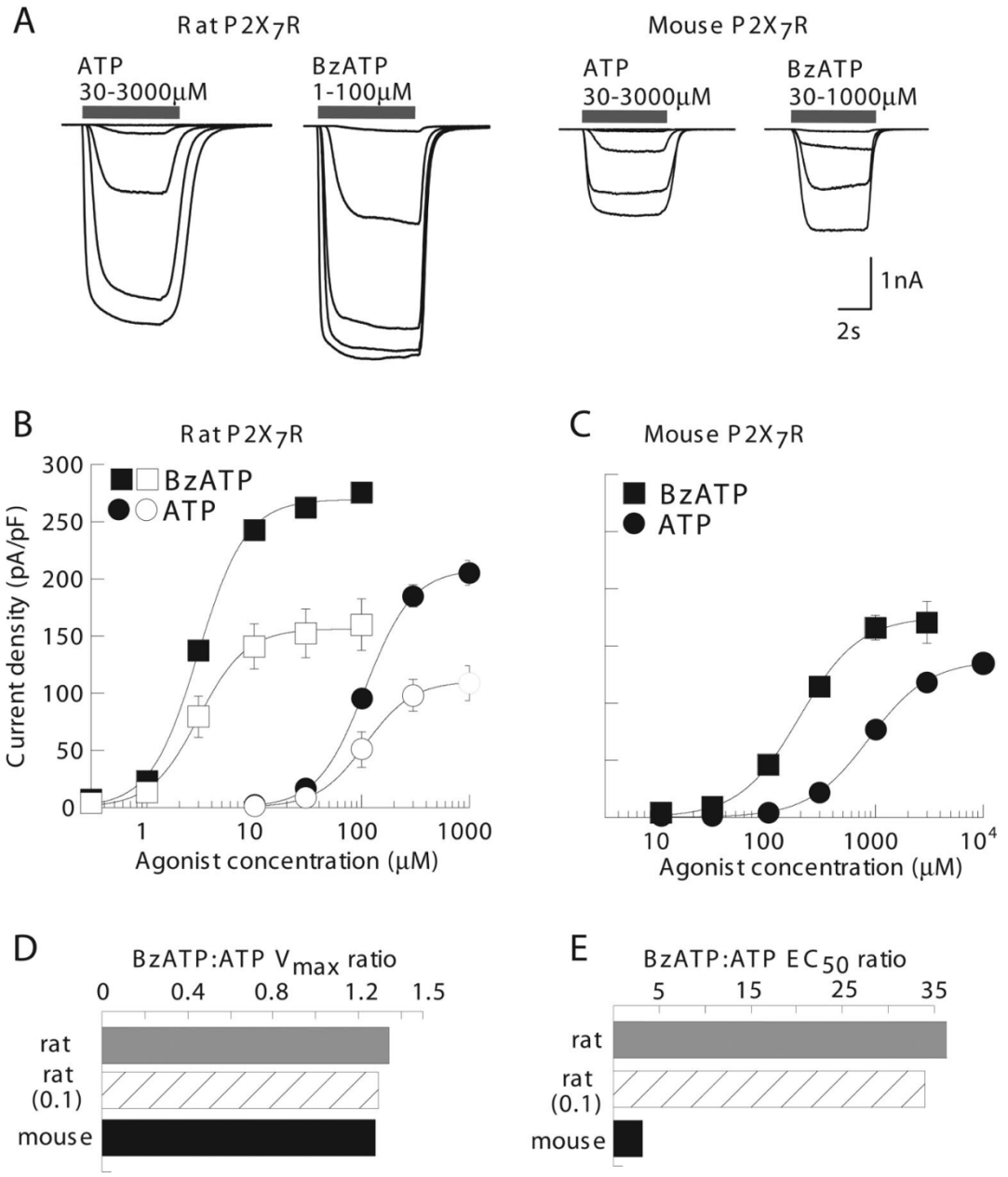
A
Rat P2X7R
ATP
30-3000µM
BzATP
1-100µM
Mouse P2X7R
ATP
30-3000µM
BzATP
30-1000µM
1nA
2s
B
Rat P2X7R
BzATP
ATP
Current density (pA/pF)
300
250
200
150
100
50
0
1
10
100
1000
Agonist concentration (µM)
C
Mouse P2X7R
BzATP
ATP
10
100
1000
10^4
Agonist concentration (µM)
D
BzATP:ATP Vmax ratio
0
0.4
0.8
1.2
1.5
rat
rat
(0.1)
mouse
E
BzATP:ATP EC50 ratio
5
15
25
35
rat
rat
(0.1)
mouse

FIGURE 3

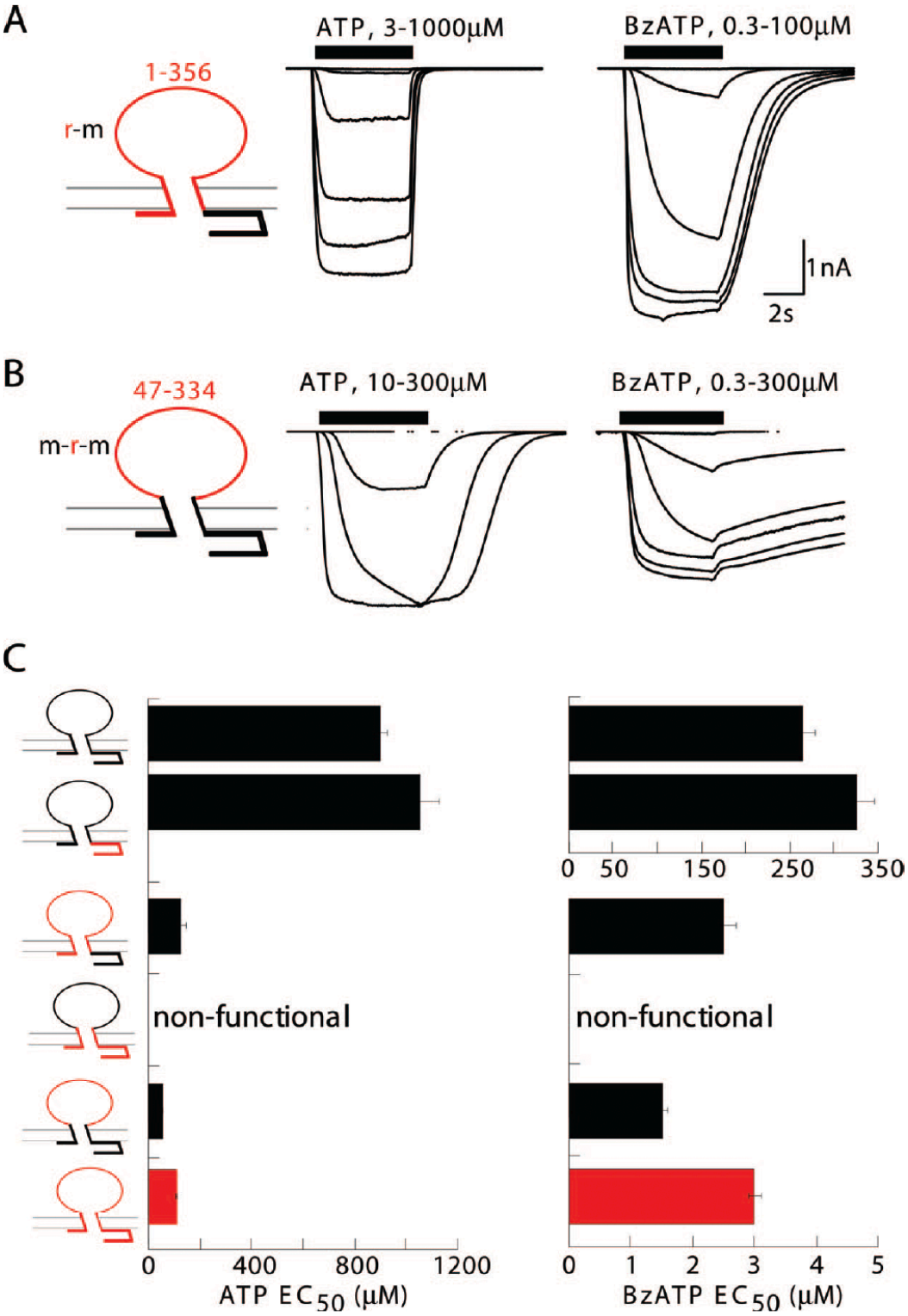
A
ATP, 3-1000µM
BzATP, 0.3-100µM
1-356
r-m
1nA
2s
B
47-334
m-r-m
ATP, 10-300µM
BzATP, 0.3-300µM
C
non-functional
non-functional
0 400 800 1200
ATP EC50 (µM)
0 50 150 250 350
0 1 2 3 4 5
BzATP EC50 (µM)

FIGURE 4

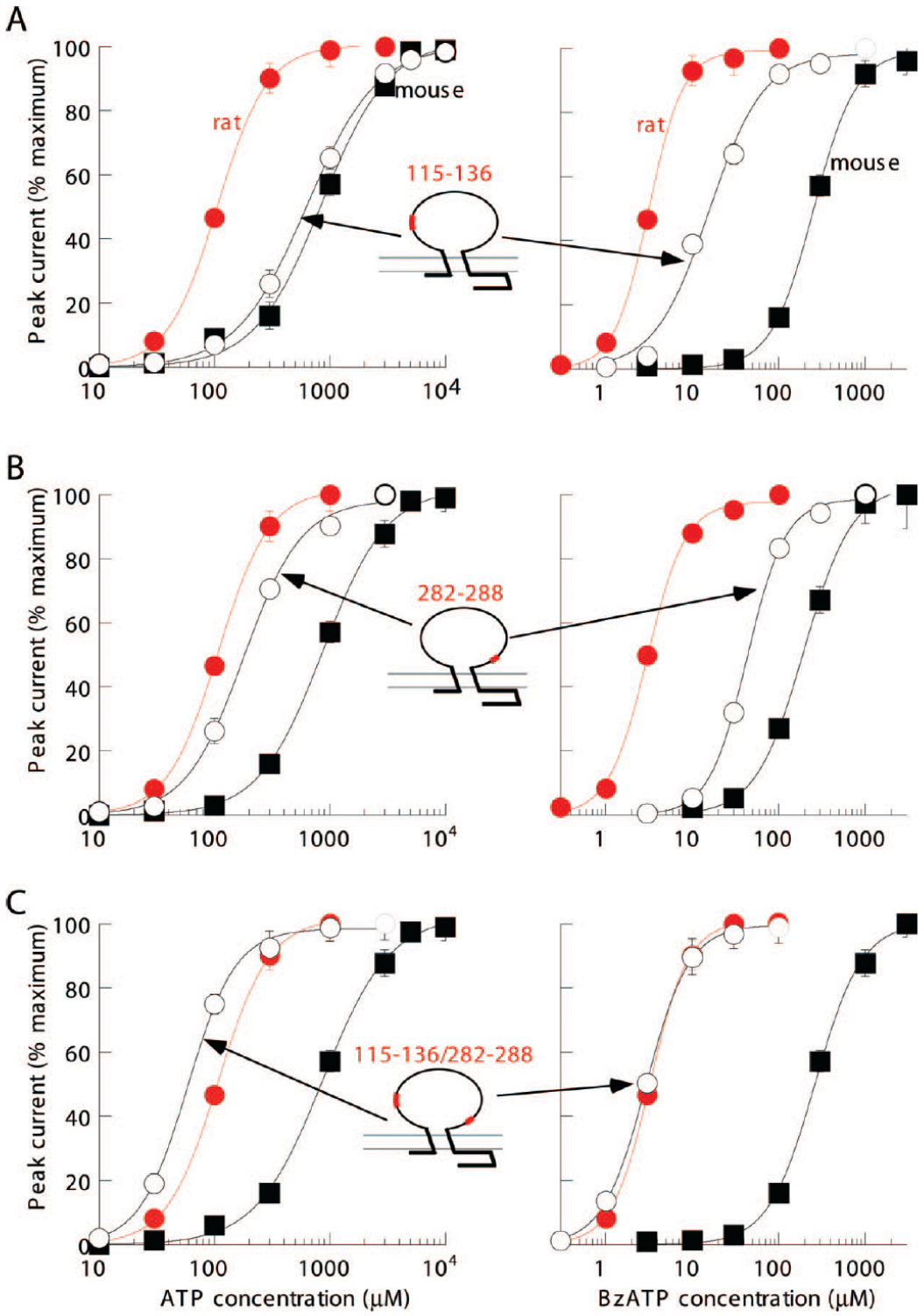
A
B
C
Peak current (% maximum)
100
80
60
40
20
0
rat
mouse
115-136
282-288
115-136/282-288
10
100
1000
10^4
1
ATP concentration (μM)
BzATP concentration (μM)

FIGURE 5

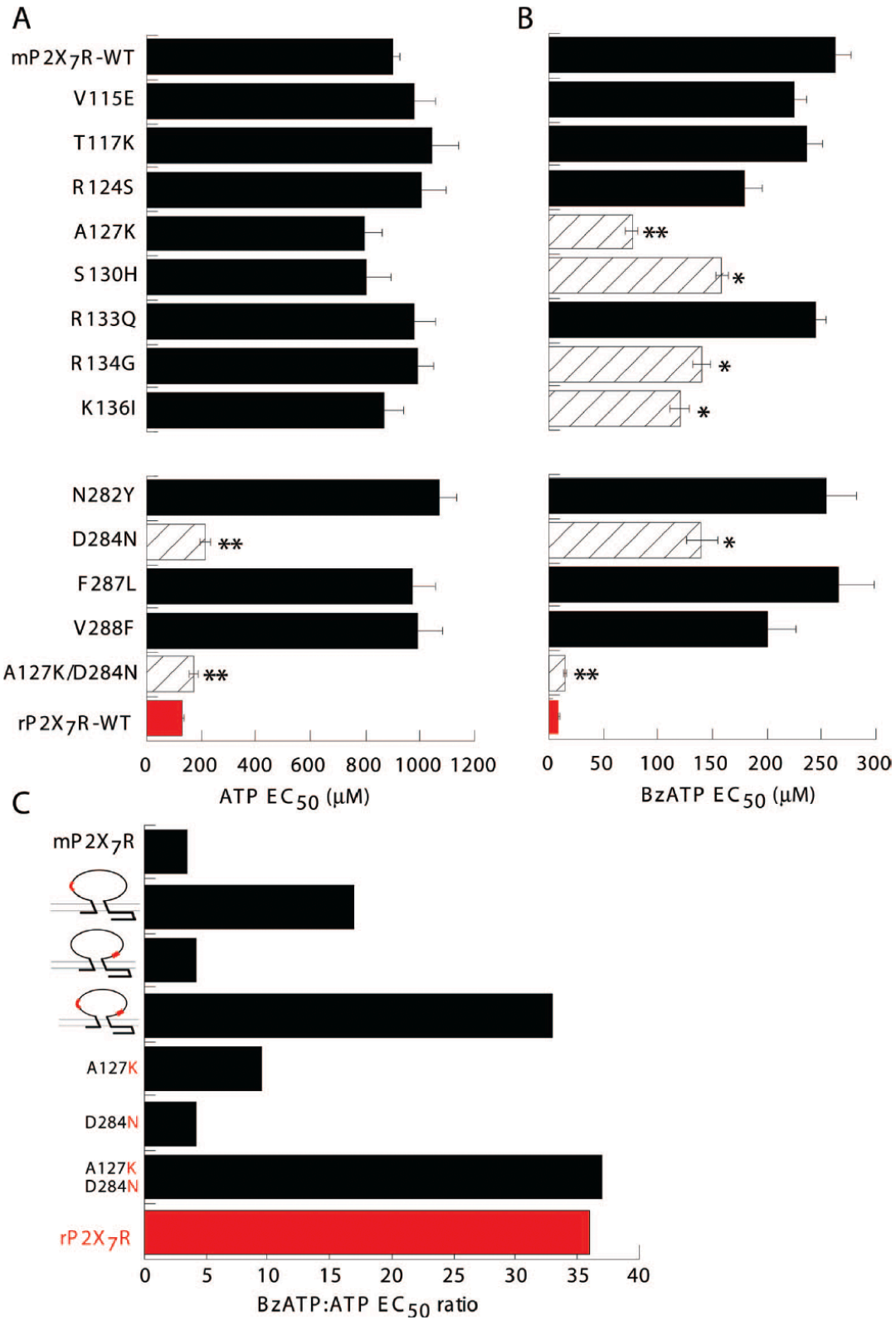
A
mP2X7R-WT
V115E
T117K
R124S
A127K
S130H
R133Q
R134G
K136I
N282Y
D284N
F287L
V288F
A127K/D284N
rP2X7R-WT
**
*
0 200 400 600 800 1000 1200
ATP EC50 (μM)
B
0 50 100 150 200 250 300
BzATP EC50 (μM)
C
mP2X7R
A127K
D284N
A127K
D284N
rP2X7R
0 5 10 15 20 25 30 35 40
BzATP:ATP EC50 ratio

FIGURE 6

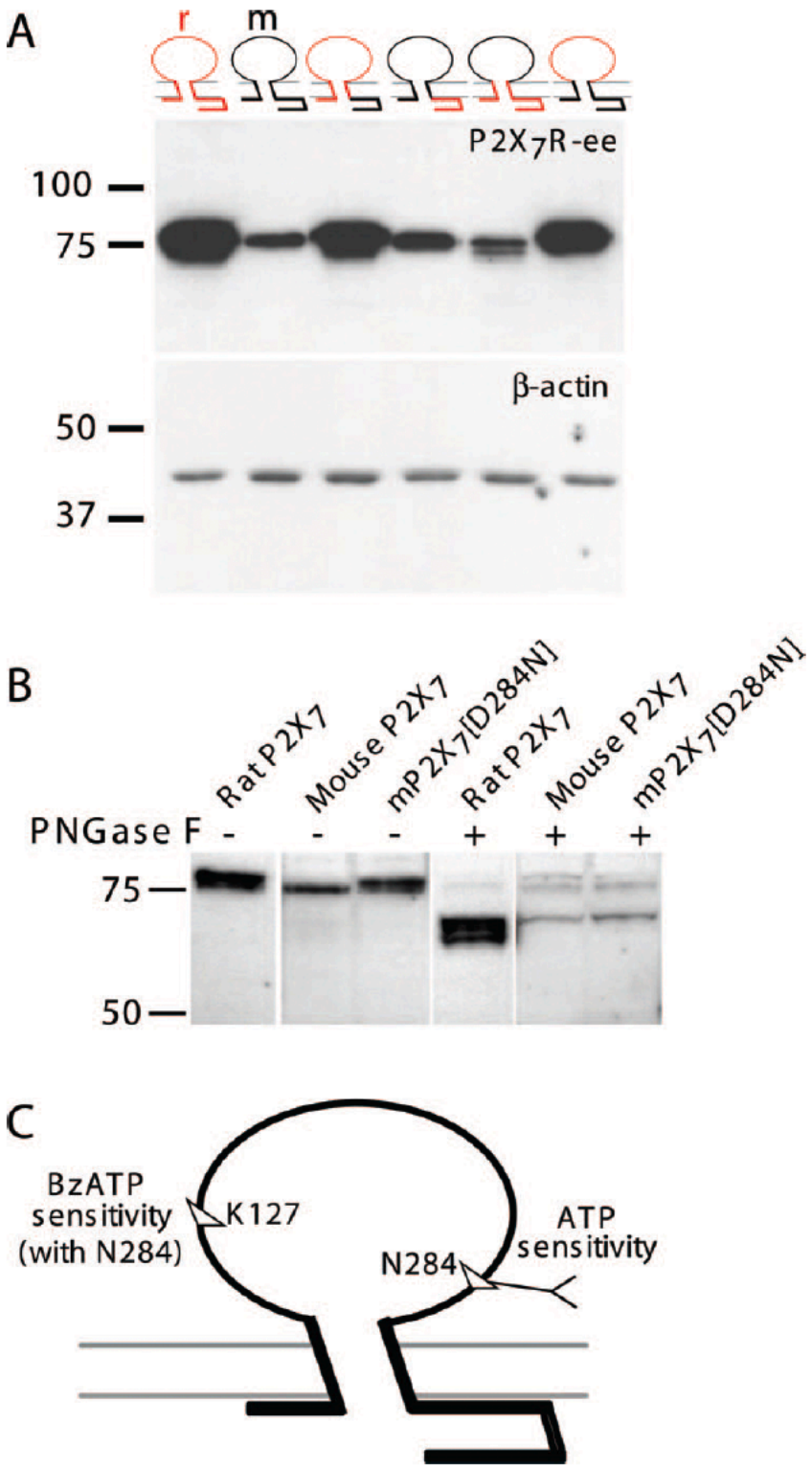
A
r
m
P2X7R-ee
100
75
β-actin
50
37
B
Rat P2X7
Mouse P2X7
mP2X7[D284N]
Rat P2X7
Mouse P2X7
mP2X7[D284N]
PNGase F - - - + + +
75
50
C
BzATP sensitivity (with N284)
K127
N284
ATP sensitivity